Searches for squarks in R_p violating SUSY

Abstract:

A search for squarks in R-parity violating supersymmetry is performed in e^+p collisions at HERA at a centre of mass energy of 320 GeV, using 99/00 H1 data corresponding to an integrated luminosity of 63 pb^{-1}. The direct production of single squarks of any generation in positron-quark fusion via a Yukawa coupling λ' is considered, taking into account R-parity violating and conserving decays of the squarks. No significant deviation from the Standard Model expectation is found. The results are interpreted in terms of constraints within various supersymmetric models and their sensitivity to the model parameters is studied in detail.

For details of the analysis please have a look at

- the publication on the similar analysis performed on 1994-1997 H1 data:
  DESY-01-021 or hep-ex/0102050
- the internal web page where all cuts, control plots and some informations are given:
  file:///afs/desy.de/user/h/haller/h1/prelim/prelim.html

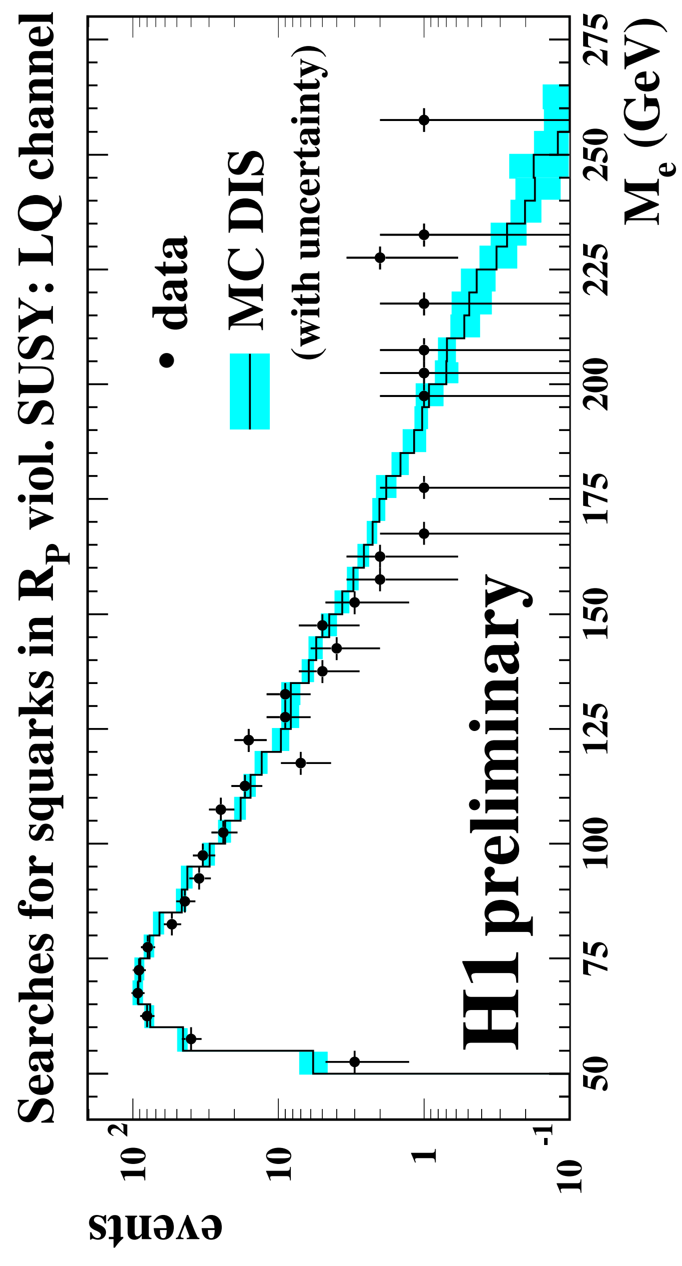

Figure 1: Mass spectrum in the electron-leptoquark channel. The mass is calculated from $M_e = \sqrt{sx}$ where s is the square of the ep centre of mass energy and x is calculated using information from the electron.

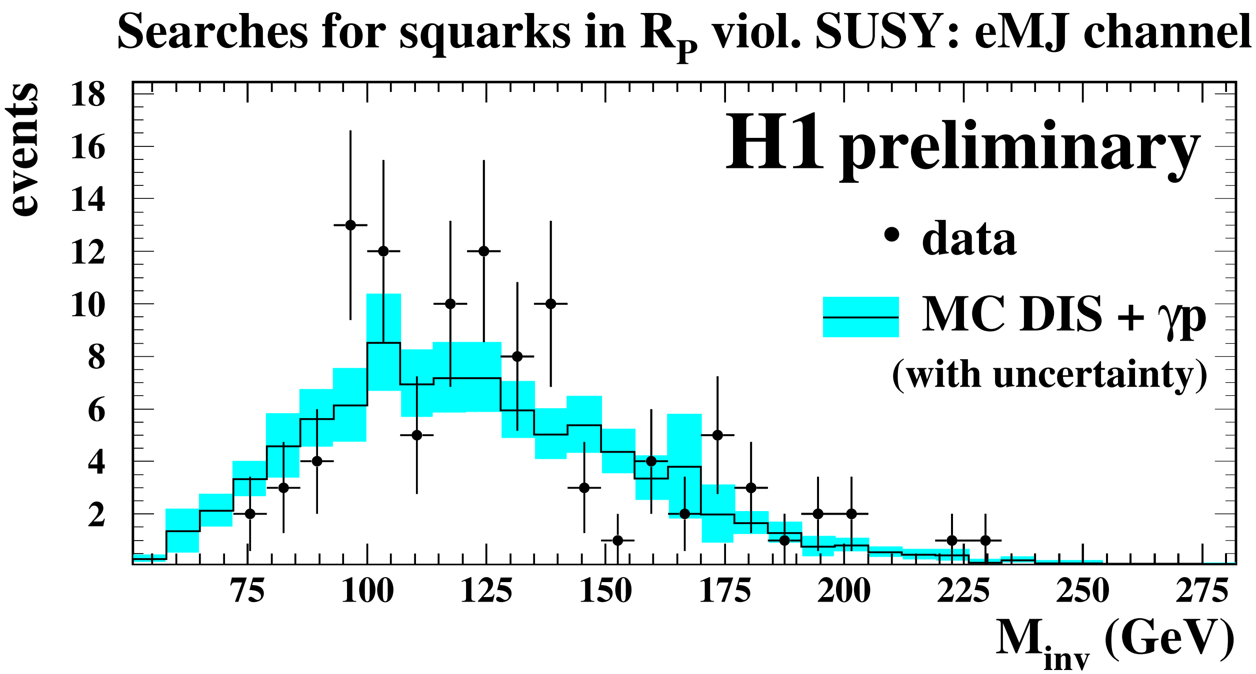

Figure 2: Mass spectrum in the decay channel with one electron and multiple jets. The reconstruction method used is as described in DESY-01-021.

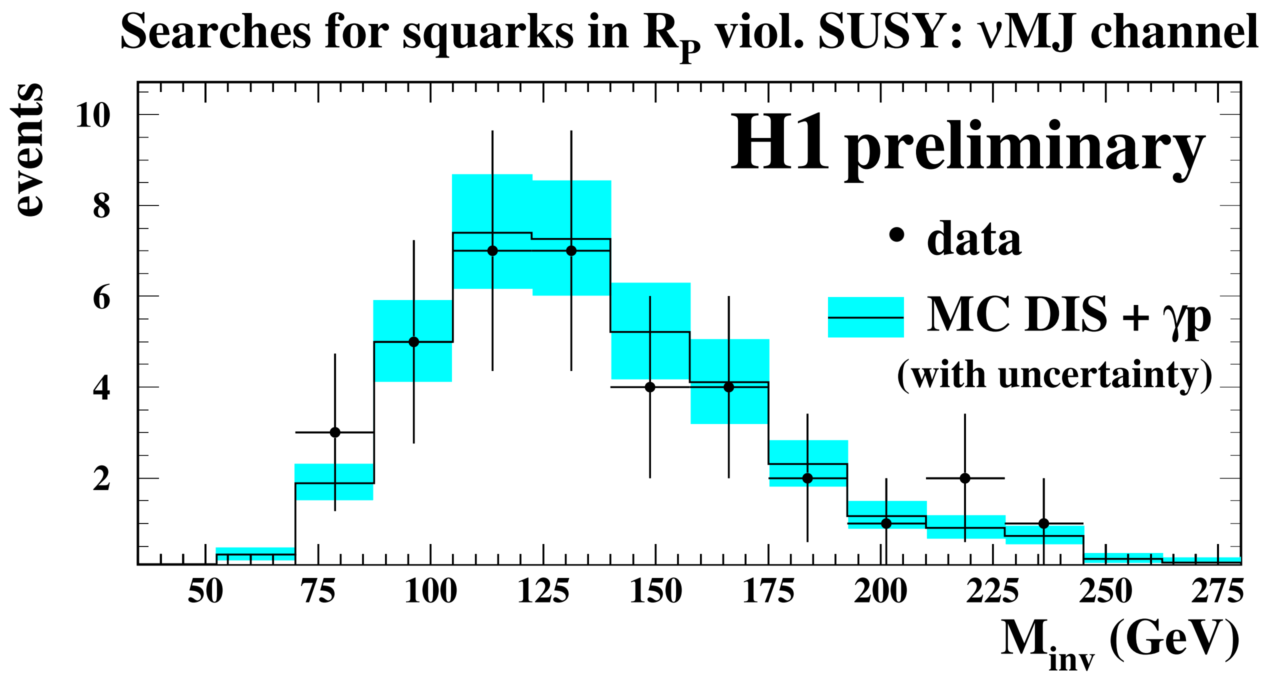

Figure 3: Mass spectrum in the decay channel with missing transverse momentum and multiple jets. The reconstruction method used is as described in DESY-01-021.

Channel	data	SM prediction
LQ	690	705.9 ± 51.3
eMJ	104	89.6 ± 14.0
e^-MJ	0	0.33 ± 0.15
eeMJ	0	0.79 ± 0.22
eμMJ	0	0.96 ± 0.26
νeMJ	0	1.7 ± 0.5
νMJ	36	36.8 ± 6.0
$\nu\mu$MJ	0	0.65 ± 0.25

Table 1: Summary of total event numbers for all channels. The selection cuts are basically the same as in DESY-01-021.

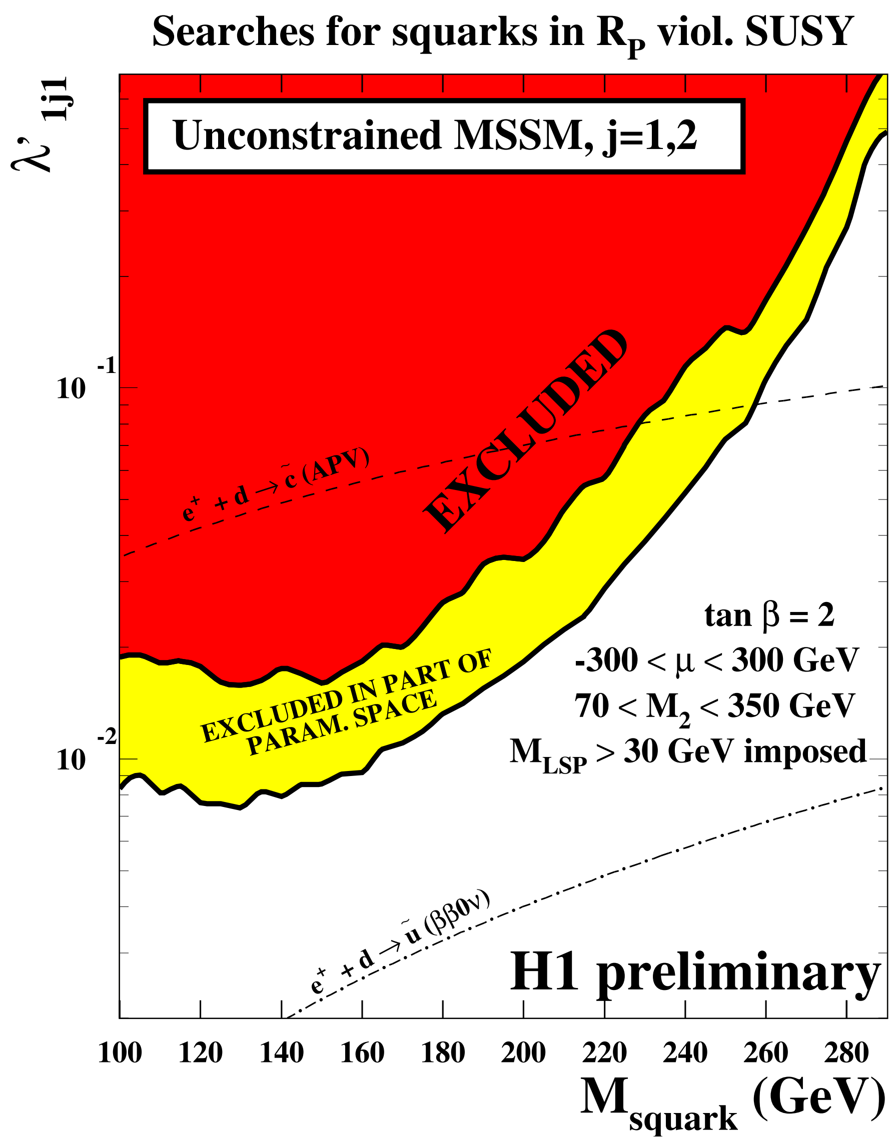

Figure 4: Limits on λ'_{1j1} $\quad j = 1, 2$ as a function of squark mass from a scan in SUSY parameter space for $\tan\beta = 2$ to study the model dependence. Shown is the strongest (yellow, grey) and the weakest (red, dark) value for the coupling limit. Compared with the analysis of 1994-1997 data, the improvement is largest at high masses, because of the increased centre-of-mass energy. The slepton masses are set to 90 GeV (about the LEP limit). The dashed-dotted line indicates the indirect bound on λ'_{111} form neutrinoless double beta decay ($\beta\beta0\nu$) assuming a gluino mass of 1 TeV. The dashed curve shows the indirect bounds from atomic parity violation (APV).

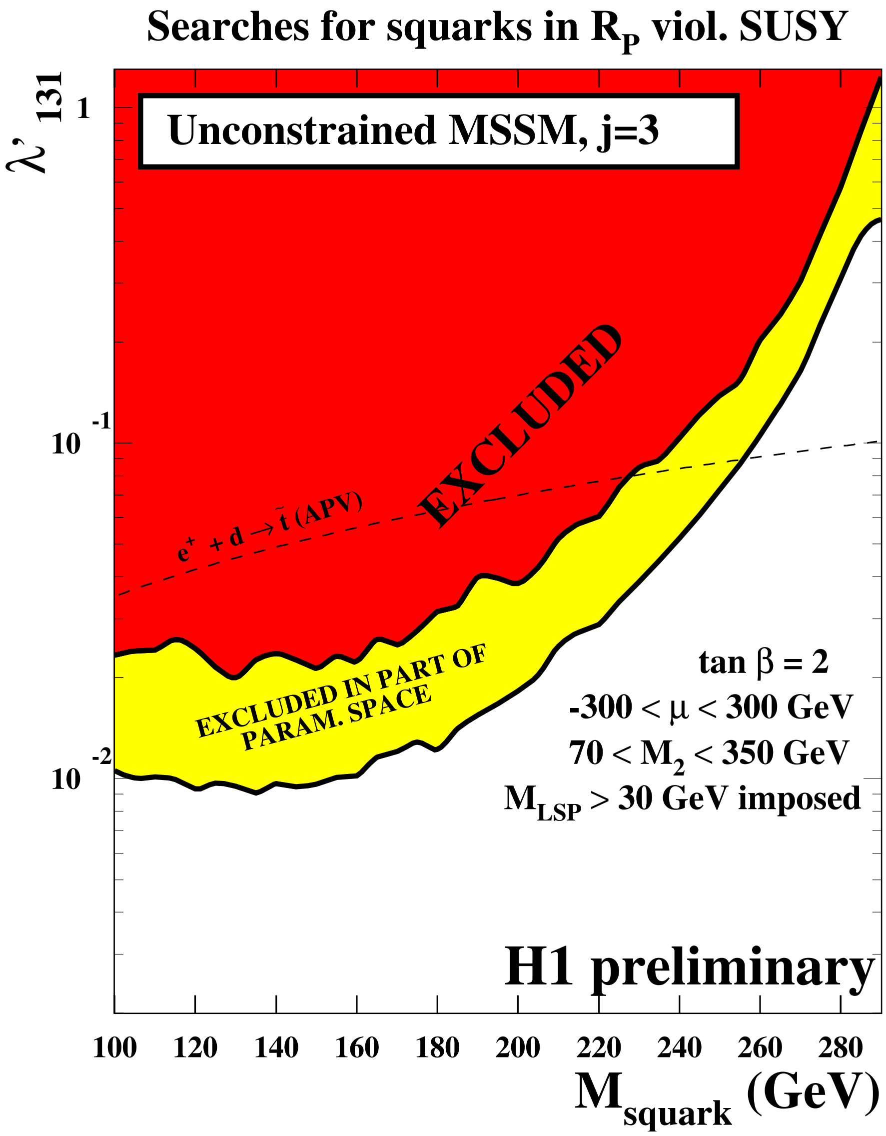

Figure 5: Limits on λ'_{1j1} $j = 3$ as a function of squark mass from a scan in SUSY parameter space for $\tan\beta = 2$. Shown is the strongest (yellow, grey) and the weakest (red, dark) value for the coupling limit. Compared with the analysis of 1994-1997 data, the improvement is largest at high masses because of the increased centre-of-mass energy. The slepton masses are set to 90 GeV (about the LEP limit). The case of $j = 3$ must be treated separately since $\lambda'_{131} \neq 0$ may lead to a top quark in the final state, for which the selection efficiencies are not known. Although most of the stop decays are in fact covered by our analysis, the efficiency was conservatively set to zero for cases with a top quark in the final state. The dashed curve shows the indirect bounds from atomic parity violation (APV).

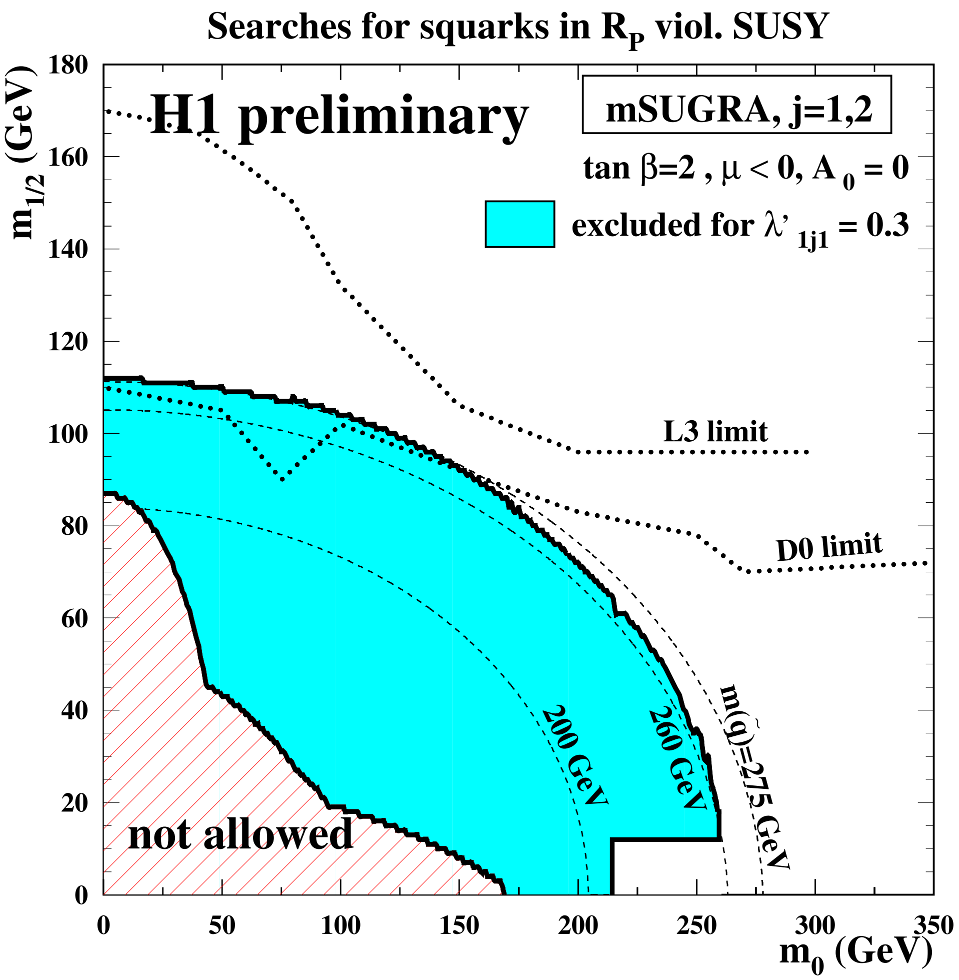

Figure 6: Limits in the minimal Super–Gravity model with $\tan\beta = 2$. Shown is the area that is not allowed (hatched) and the area that is excluded by H1. Curves of constant squark mass are also shown. Compared to the analysis of 1994-1997 data, we improve the limits by 15 GeV for the squark mass, now reaching 275 GeV for a coupling of electromagnetic strength. The regions below the dashed curves are excluded by D0 and L3 respectively.

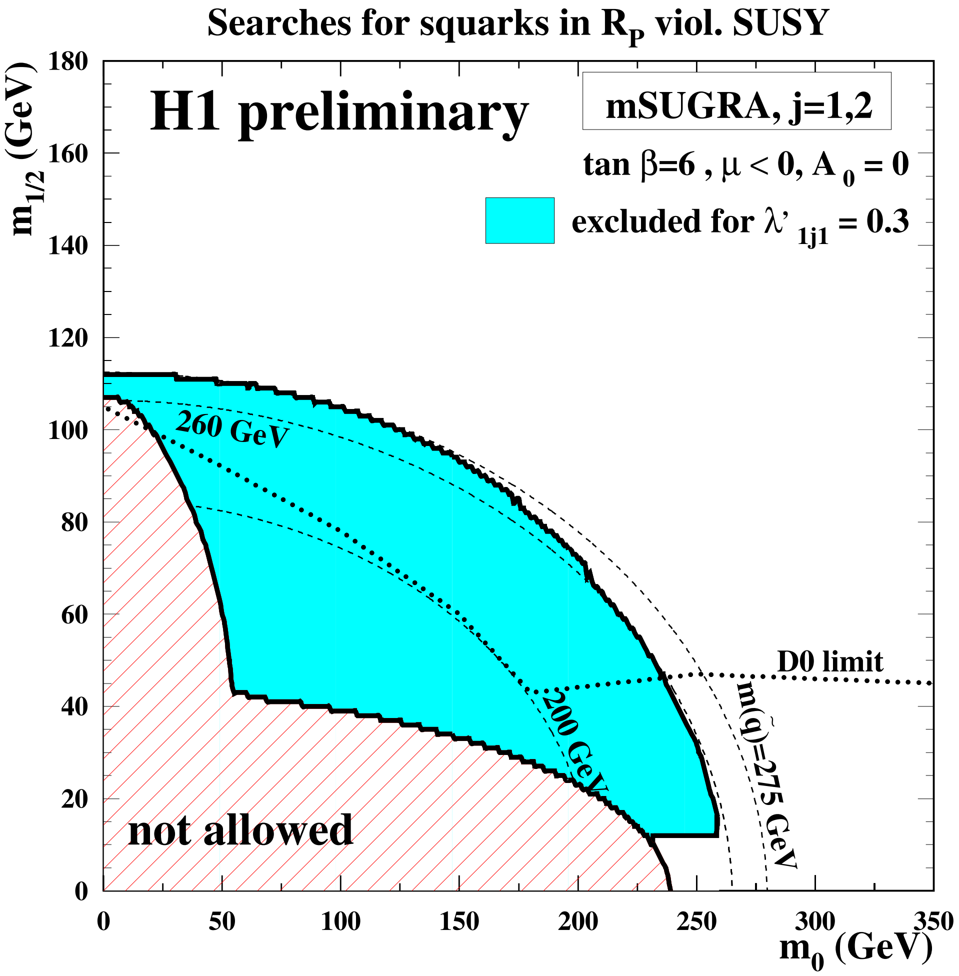

Figure 7: Limits in the minimal Super–Gravity model with $\tan\beta = 6$. Shown is the area that is not allowed (hatched) and the area that is excluded by H1. Curves of constant squark mass are also shown. Compared to the analysis of 1994-1997, we improve the limits by 15 GeV for the squark mass, now reaching 275 GeV for a coupling of electromagnetic strength.

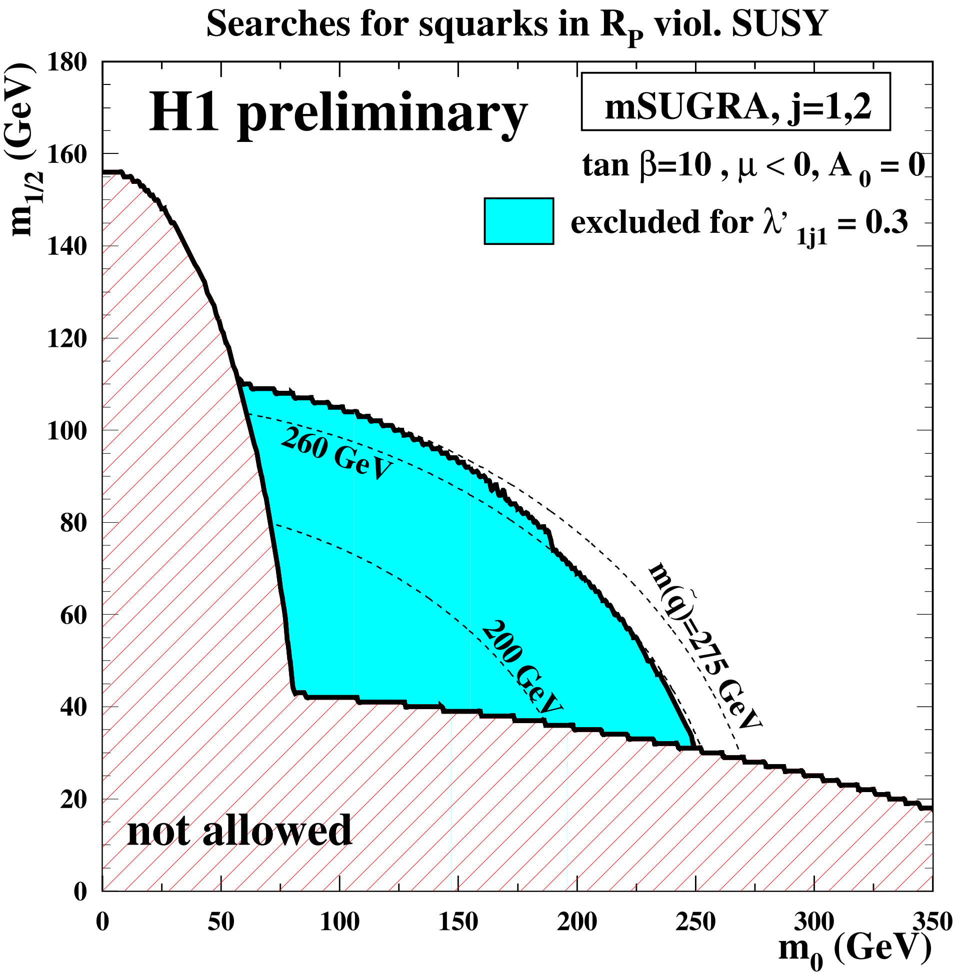

Figure 8: Limits in the minimal Super–Gravity model with $\tan\beta = 10$. Shown is the area that is not allowed (hatched), the area that is excluded by H1 and curves of constant squark mass. We now give a limit for $\tan\beta = 10$ since recent Higgs searches at LEP suggest a large value of $\tan\beta$.

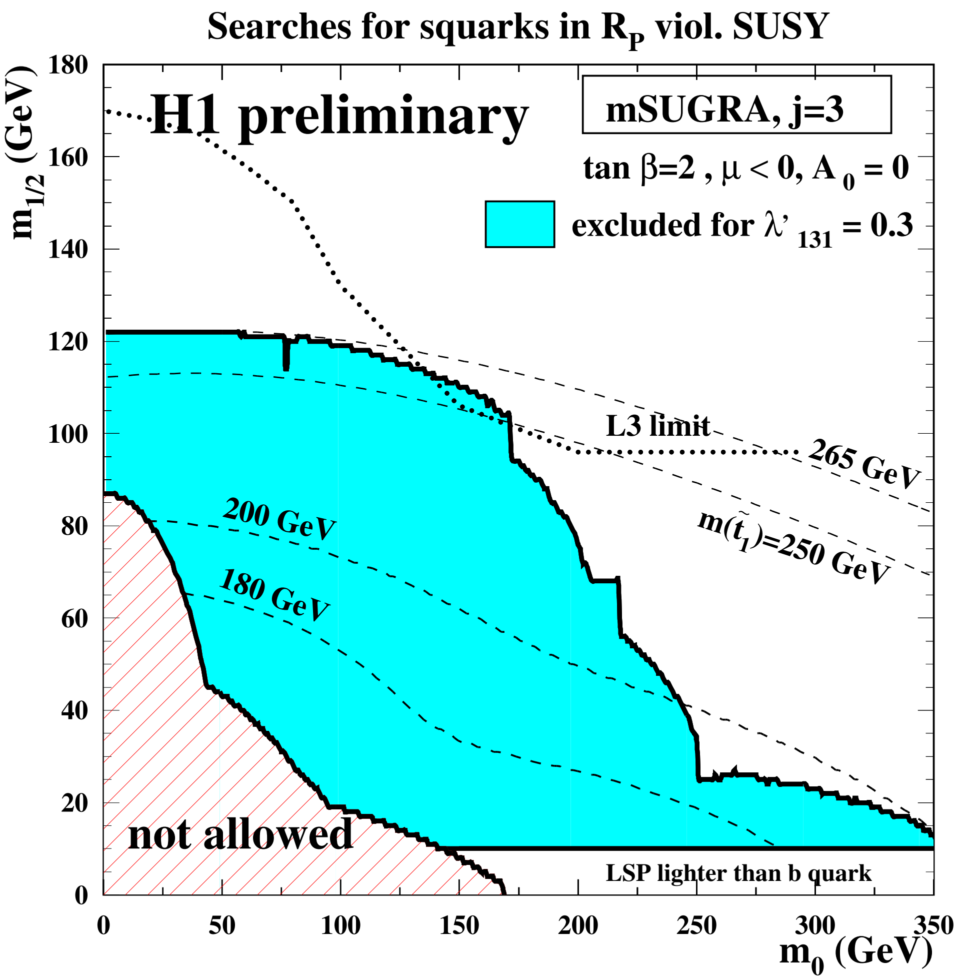

Figure 9: Limits in the minimal Super–Gravity model for $\tan\beta = 2$ with $j = 3$, which is treated separately for the reasons explained in the caption of figure 5. Shown is the area that is not allowed (hatched), the area that is excluded by H1 and curves of constant stop mass. The sharp edges are well understood, mostly corresponding to regions where the gaugino masses fall below 30 GeV and our efficiency is set to zero. We are sensitive to this region, but we did not consider it, since gaugino masses below 30 GeV are excluded by LEP searches. For more details see DESY-01-021.

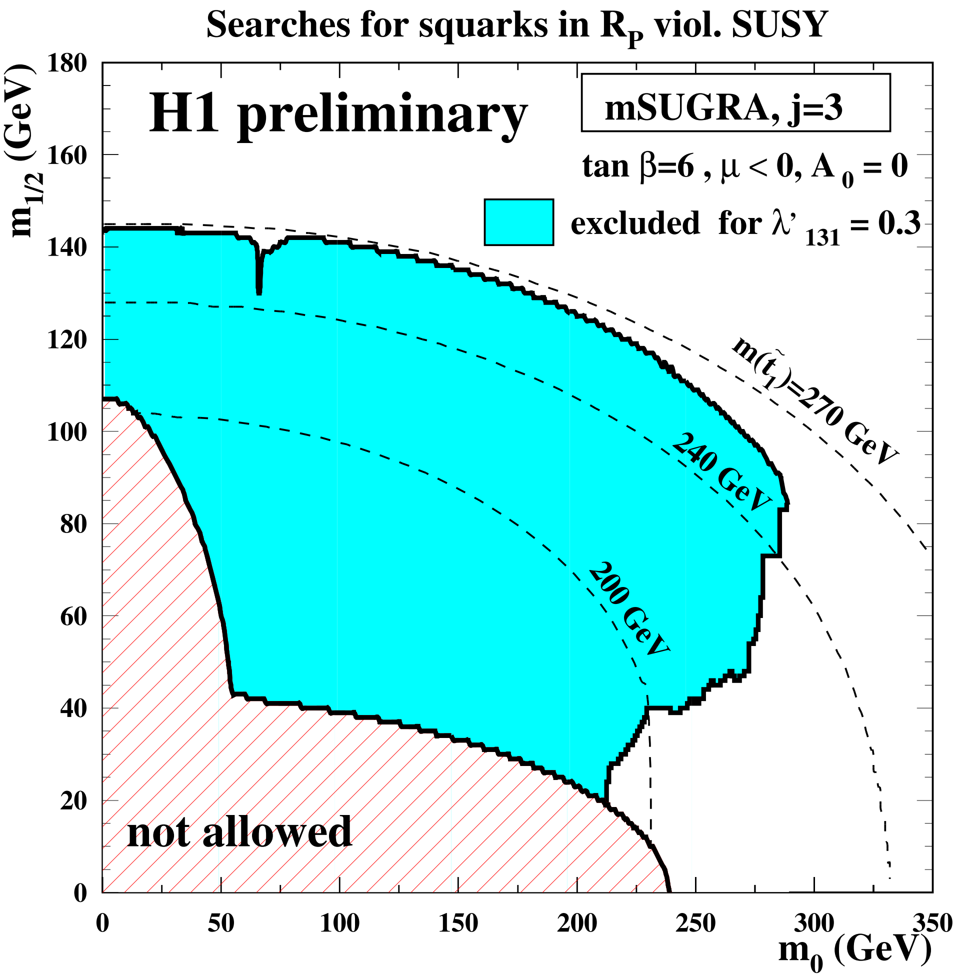

Figure 10: Limits in the minimal Super–Gravity model for $\tan\beta = 6$ with $j = 3$. Shown is the area that is not allowed (hatched), the area that is excluded by H1 and curves of constant stop mass.

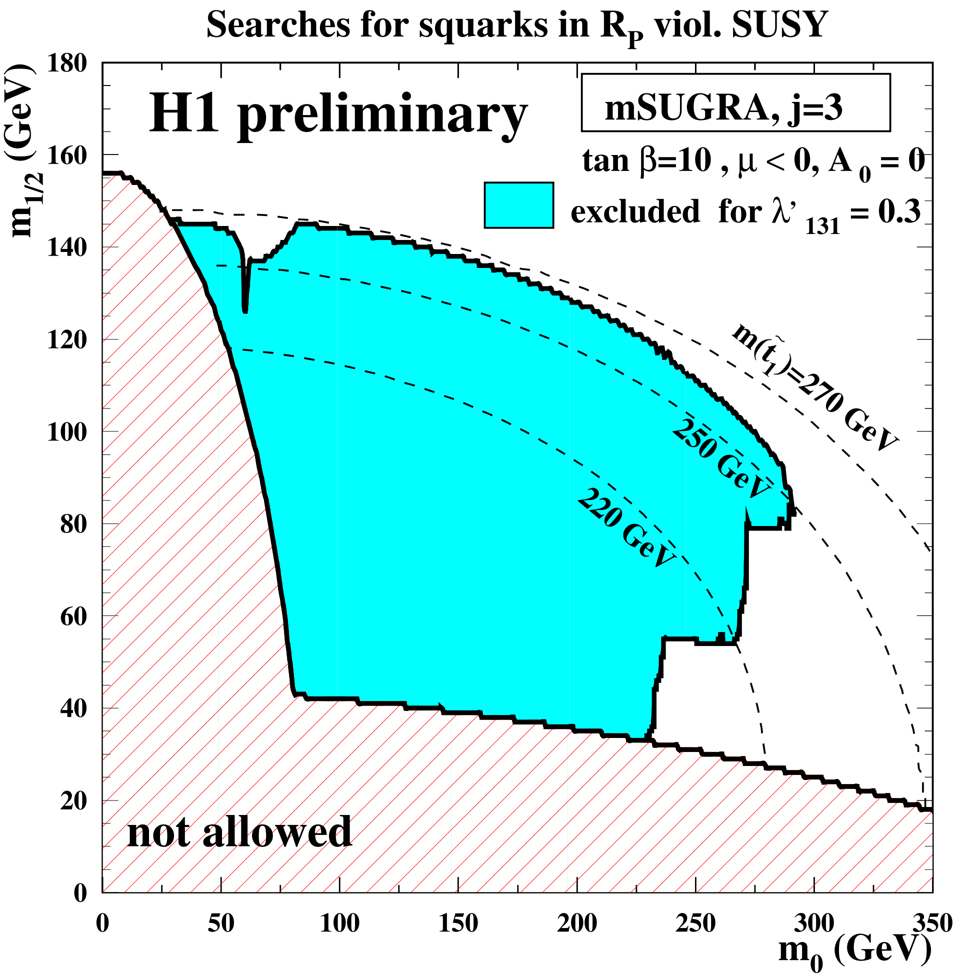

Figure 11: Limits in the minimal Super–Gravity model for $\tan\beta = 10$ with $j = 3$. Shown is the area that is not allowed (hatched), the area that is excluded by H1 and curves of constant stop mass.